

Toward defeating diffraction and randomness for laser beam propagation in turbulent atmosphere

Pavel M. Lushnikov and Natalia Vladimirova¹

¹*Department of Mathematics and Statistics, University of New Mexico, USA*

compiled: August 10, 2018

A large distance propagation in turbulent atmosphere results in disintegration of laser beam into speckles. We find that the most intense speckle approximately preserves both the Gaussian shape and the diameter of the initial collimated beam while losing energy during propagation. One per 1000 of atmospheric realizations produces at 7km distance an intense speckle above 20% of the initial power. Such optimal realizations create effective extended lenses focusing the intense speckle beyond the diffraction limit of vacuum propagation. Atmospheric realizations change every several milliseconds. We propose to use intense speckles to greatly increase the time-averaged power delivery to the target plane by triggering the pulsed laser operations only at times of optimal realizations. Resulting power delivery and laser irradiance at the intense speckles well exceeds both intensity of diffraction-limited beam and intensity averaged over typical realizations.

OCIS codes: (010.1330) Atmospheric turbulence; (010.1290) Atmospheric optics; (190.4370).
<http://dx.doi.org/10.1364/XX.99.099999>

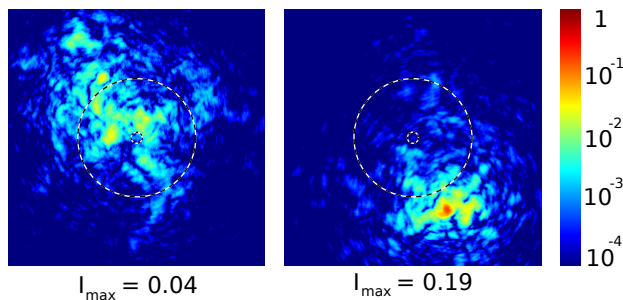


Fig. 1. (Color online) Distribution of laser irradiance I in transverse plane (only 69x69 cm central part of target screen is shown) after $L = 7$ km propagation of the collimated Gaussian laser beam with the waist $w_0 = 1.5$ cm and the maximal intensity $I_{max} = 1$ through the turbulent atmosphere in the strong scintillation regime with $\sigma_I = 3.3$. Left panel: a typical atmospheric turbulence realization with $I_{max} = 0.04$ (61% of atmospheric realizations produce higher I_{max}). Right panel: a rare realization with $I_{max} = 0.19$ (0.16% realizations produce higher I_{max}). Dashed circles show w_0 and the waist of diffraction limited beam propagated in vacuum. The initial Gaussian beam disintegrates into several speckles with the width of the most intense speckle being about w_0 . The intense speckles on left and right panels carry 4% and 19% of the total laser power, respectively.

Laser beam propagation through turbulent atmosphere results in disintegration of laser beam into speckles at the distances exceeding several kilometers (strong irradiance fluctuation regime) [1], see Fig. 1 with examples of such propagation. At smaller distances (weak irradi-

ance fluctuation regime) classic perturbative approaches well describe modification of laser beam propagation due to turbulence [2, 3], while statistically averaged beam propagation in strong scintillation regimes is addressed through semi-heuristic theory [4]. The strength of the fluctuations of the irradiance I (laser beam intensity) at the target plane is characterized by the scintillation index $\sigma_I \equiv \langle I^2 \rangle / \langle I \rangle^2 - 1$. Here and below by $\langle \dots \rangle$ we denote an average over the ensemble of atmospheric turbulence realizations. It was shown in Ref. [5] that a significant fraction of deviation between theoretical value of σ_I [4] and simulations is due to rare large fluctuations of laser beam intensity. Here we study the structure of large fluctuations and propose to use them for the efficient delivery of laser energy over long distances by triggering the pulse laser operations only during the times of such rare fluctuations. Rare fluctuations which carry $\gtrsim 19\%$ of initial power, as in Fig. 1, occurs in 0.16% realizations, and 0.1% realizations carry $\gtrsim 21\%$ of initial power. A temporal rate of change in atmospheric realizations is affected by atmosphere conditions. In typical conditions new atmospheric realization could occur each ~ 10 ms [5]. Thus waiting for the optimal realization might take several seconds.

A propagation of a monochromatic beam with a single polarization through the turbulent media is described by the linear Schrödinger equation (LSE) (see e.g. [2, 3]):

$$i \frac{\partial}{\partial z} \psi + \frac{1}{2k} \nabla_{\perp}^2 \psi + k n_1(\mathbf{r}, z) \psi = 0. \quad (1)$$

Here the beam is aligned along z -axis, $\mathbf{r} \equiv (x, y)$ are the transverse coordinates, $\psi(\mathbf{r}, z)$ is the envelope of the elec-

tric field, $\nabla_{\perp} \equiv \left(\frac{\partial}{\partial x}, \frac{\partial}{\partial y}\right)$, $k = 2\pi n_0/\lambda_0$ is the wavenumber in medium, λ_0 is the wavelength in the vacuum, $n = n_0 + n_1$ is the linear index of refraction with the average value $n_0 = \langle n \rangle$ and the fluctuation $n_1(\mathbf{r}, z, t)$. Time t does not explicitly enters Eq. (1), thus serving as parameter distinguishing different atmospheric realizations so below we omit t in arguments of all functions.

Linear absorption (results in exponential decay of laser intensity with propagation distance) is straightforward to include into Eq. (1). Kerr nonlinearity can be also added to Eq. (1) resulting in nonlinear Schrödinger Eq. which describes the catastrophic self-focusing (collapse) for laser powers P above critical power P_c ($P_c \sim 3\text{GW}$ for $\lambda_0 = 1064\text{nm}$) [6–8] and multiple filamentation for $P \gg P_c$ [9]. At distances well below the nonlinear length, one can consider Kerr nonlinearity as perturbation (see e.g. Ref. [10]) combining it with the effect of atmospheric turbulence. Nonlinear beam combining in atmosphere can be also considered to fight with turbulence [11, 12]. Such nonlinear analysis is however beyond the scope of this Letter.

We solve Eq. (1) by the standard method of random phase screens [4] which is based on the approximation of statistically independent optical pulse phase fluctuations at each screen [3]. This method is a version of split-step numerical method [13, 14] which separates Eq. (1) into the exactly solvable refraction, $\partial_z \psi^R = ikn_1(\mathbf{r}, z)\psi^R$, and diffraction, $\partial_z \psi^D = \frac{i}{2k} \nabla_{\perp}^2 \psi^D$, parts. The exact solutions at the distance Δz are given by $\psi^R(\mathbf{r}, z + \Delta z) = \psi^R(\mathbf{r}, z) \exp(iS)$ and $\hat{\psi}_{k_{\perp}}^D(z + \Delta z) = \hat{\psi}_{k_{\perp}}^D(z) (-i \frac{k_{\perp}^2}{2k} \Delta z)$, respectively. Here $S \equiv k \int_z^{z+\Delta z} n_1(\mathbf{r}, z') dz'$ is the phase shift and $\hat{\psi}_{k_{\perp}}^D \equiv (2\pi)^{-2} \int \psi(\mathbf{r}, z) e^{-i\mathbf{r} \cdot \mathbf{k}_{\perp}} d\mathbf{r}$ is the Fourier transform (FT) for the transverse wavevector $\mathbf{k}_{\perp} = (k_x, k_y)$. Sequential combining both solutions at each step Δz (requires performing both FT and inverse FT), while decreasing Δz ensures convergence to the solution of Eq. (1).

The method of random phase screen approximates FT of the phase shift at the refraction step as $\hat{S}_{k_{\perp}} = \hat{\xi}_{k_{\perp}} k \sqrt{2\pi \hat{\Phi}_{k_{\perp}} \Delta z}$, where $\hat{\Phi}_{k_{\perp}} \equiv \hat{\Phi}_{k_{\perp}, \kappa=0} \equiv (2\pi)^{-3} \int D(\mathbf{r}, z) e^{-i(\mathbf{r} \cdot \mathbf{k}_{\perp} + \kappa z)}|_{\kappa=0} d\mathbf{r} dz$ is the FT over $\rho \equiv (\mathbf{r}, z)$ of the structure function, $D(\rho) \equiv \langle [n_1(\mathbf{r}, z) - n_1(\mathbf{0}, 0)]^2 \rangle$, evaluated at the zero component $\kappa = 0$ of the wavevector in z direction [15]. The Kolmogorov-Obukhov law $D(\rho) \simeq C_n^2 \rho^{2/3}$ is valid for the atmospheric turbulence (at $l_0 \ll \rho \ll L_0$) which implies $\hat{\Phi}_{k_{\perp}} = 0.033 C_n^2 k_{\perp}^{-11/3}$, $|\mathbf{k}_{\perp}| = k_{\perp}$ [15]. Here l_0 is the inner scale of turbulence, typically a few mm, and L_0 is the outer scale typically ranging from hundred meters to kilometers. The modification of $\hat{\Phi}_{k_{\perp}}$ for both $k_{\perp} \gtrsim 2\pi/L_0$ and $k_{\perp} \lesssim 2\pi/L_0$ is straightforward to implement [4, 15]. We found in agreement with Ref. [5], that the simplest numerical cutoff described below does not affect the results of simulation for our range of parameters. These parameters include the size of the square computational domain (the trans-

verse screen size) $L = L_x = L_y = 276.5$ cm with the uniformly distributed $N \times N$ points in that domain and $N = 1024$. It implies that $-\pi N/L \leq k_x(k_y) \leq \pi N/L$ which defines the upper cut-off in k_{\perp} variable, while the elementary step $\Delta k = 2\pi/L$ of the numerical grid $\mathbf{k}_{j_{\perp}} \equiv \Delta k(j_x, j_y)$, $-N/2 \leq j_x(j_y) \leq N/2$ in \mathbf{k}_{\perp} determines the lower cut-off. Also $\hat{\xi}_{\mathbf{k}_{\perp}}$ are the uncorrelated complex Gaussian random variables on the grid $\mathbf{k}_{j_{\perp}}$, such that $\langle \hat{\xi}_{\mathbf{k}_{j_{\perp}}} \rangle = \langle \hat{\xi}_{\mathbf{k}_{j_1 \perp}} \hat{\xi}_{\mathbf{k}_{j_2 \perp}}^* \rangle = 0$ for $\mathbf{j}_1 \neq \mathbf{j}_2$ and $\langle |\hat{\xi}_{\mathbf{k}_{j_{\perp}}}|^2 \rangle = (\Delta k)^{-2}$. Here $*$ means complex conjugation and the real values of S are ensured by the condition $\hat{\xi}_{-\mathbf{k}_{j_{\perp}}} = \hat{\xi}_{\mathbf{k}_{j_{\perp}}}^*$. This numerical method is similar to Ref. [5], except that Ref. [5] used top-hat probability density function (PDF) for $\hat{\xi}_{\mathbf{k}_{j_{\perp}}}$ instead of Gaussian PDF. We also verified that top-hat PDF produces essentially the same results (nearly visually indistinguishable on the plots below) in comparison with Gaussian PDF which is expected from the central limit theorem [16] for $N \gg 1$.

Physical parameters for our simulations are $\lambda = 1.064\mu\text{m}$, the propagation distance $z_{\text{final}} = 7$ km with $\Delta z = 350\text{m}$, $C_n^2 = 10^{-14} \text{m}^{-2/3} = 4.64 \times 10^{-16} \text{cm}^{-2/3}$ and a collimated input Gaussian laser beam $\psi(\mathbf{r}, 0) = \exp(-r^2/w_0^2)$ with the waist $w_0 = 1.5$ cm of unit intensity. Examples of simulations are shown in Fig. 1. The size of ensemble is typically $4 \cdot 10^4$ atmospheric realizations. The averaged maximum of irradiance $\langle I_{\text{max}} \rangle = 5.10433 \cdot 10^{-2}$ (here I_{max} is the maximum intensity in the target plane) and the averaged irradiance $I_{\text{center}} = 2.86788 \cdot 10^{-3}$ at the center of the target plane with $z_{\text{final}} = 7$ km. Increase of either C_n^2 or w_0 requires decrease of Δz to keep high numerical precision.

It was shown in Ref. [5] that the accurate calculation (or measurement from experiment) of σ_I requires the ensemble of $\gtrsim 10^5$ realizations (because of giant fluctuations of laser intensity) which is unpractical because atmospheric conditions are usually not stationary at the timescale required for measurements of such large ensembles (hours), i.e. the time dependence of C_n becomes essential. We argue that in this case σ_I turns to be of limited usefulness because it assumes the approximation of stationary stochastic process which is not valid due to the time dependence of C_n . Instead, we focus on the study of individual large fluctuations of laser intensity which qualitatively could be interpreted as looking into optimal realizations of atmospheric turbulence through the optimal fluctuation theory. That idea was pioneered in Ref. [17] for condensed matter, reinvented in field theory in Ref. [18] and found in many applications ranging from fluid turbulence to [19–21] to nonlinear optics [9, 22, 23].

We identified that the optimal laser fluctuation at large propagation distance $z \gtrsim 3$ km is reasonably well approximated by the Gaussian beam (we called it optimal beam (OB) below) in the general approximate form $\psi_{\text{optimal}}(\mathbf{r}, z) = I_{\text{max}}(z)^{1/2} \exp(-[\mathbf{r} - \mathbf{r}_0(z)]^2/w(z)^2 + i[\mathbf{r} - \mathbf{r}_0(z)]^2 \alpha(z) + i\mathbf{k}_{0\perp}(z) \cdot \mathbf{r} + i\phi(z))$. Here a maxi-

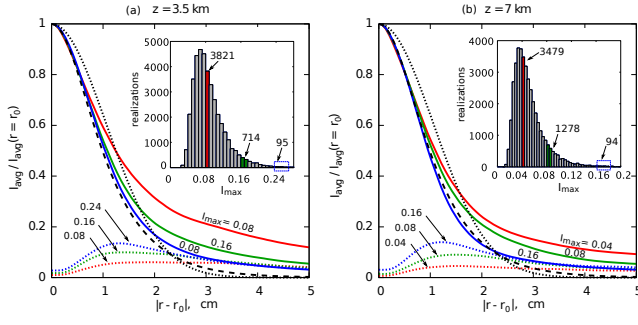


Fig. 2. (Color online) Averaged intensity profiles $I_{avg}(\mathbf{r})$ of OB centered at the location $\mathbf{r} = \mathbf{r}_0$ of intensity maximum, $I(\mathbf{r} = \mathbf{r}_0) = I_{max}$, for propagation to $z = z_{final} = 3.5$ km and 7 km. Each solid line is normalized to 1 at maximum and represents averaging over angles and over 50 OB realizations with the same final value of $I_{max}(z_{final})$. The final value is chosen within the corresponding bins (the bin width is 0.1 of I_{max}) of the histograms for $I_{max}(z_{final})$ realizations in the insets. The bins are selected near the maximum of PDF of $I_{max}(z_{final})$, in the tail and the far tail. Total number of realizations in each histogram is $4 \cdot 10^4$ (the total number of realizations in each beam is listed in the inset). The standard deviation of OB profiles are shown by corresponding short-dashed lines. Dotted line represents the initial Gaussian beam and thick dashed line shows $I = 1/\cosh(2|\mathbf{r} - \mathbf{r}_{max}|/w_0)$ for comparison. Typically, the waist of OB is $\sim 20\%$ narrower than w_0 . Similar results were also obtained in simulations with $w_0 = 3$ cm.

imum of intensity, $I_{max}(z)^{1/2}$, is located at the OB center, $\mathbf{r} = \mathbf{r}_0(z)$, the OB tilt is determined by $\mathbf{k}_{0\perp}$ and the OB waist $w(z)$ fluctuates with the propagation distance z . Also $\phi(z)$ is the fluctuating phase shift and $\alpha(z)$ determines a fluctuating curvature of OB front. Fig. 2 shows zoom into several OB realizations all centered at $\mathbf{r} = \mathbf{r}_0(z)$ with amplitude rescaled to one. It is seen that the averaged rescaled intensity profiles $I_{avg}(\mathbf{r})/I_{avg}(\mathbf{r} = \mathbf{r}_0)$ of these OBs are reasonably well match of the initial beam $|\psi(\mathbf{r}, 0)|$ with $w(z) \approx w_0$ and a typical deviation of $\sim 20\%$. Fig. 3a shows that $\mathbf{r}_0(z)$ experiences the accelerated random walk $|\mathbf{r}_0(z)| \propto z^{3/2}$ due to random Gaussian fluctuations of $\mathbf{k}_{0\perp}(z)$ from $S(\mathbf{r})$.

Note that OB appears only after the disintegration of the initial Gaussian beam into speckles. It is seen in Fig. 3b that at small propagation distance, $z \lesssim 1$ km (propagation in weak irradiance fluctuation regime), the maximum irradiance I_{max} approximately follows the diffraction limited result $I_{max,diff} = I_0(1 + z^2/z_R^2)^{-1}$, $z_R = kw_0^2/2$, while at larger distance $2 \text{ km} \lesssim z \lesssim 3 \text{ km}$ propagation in moderate irradiance fluctuation regime) I_{max} significantly deviates from $I_{max,diff}$. At the same range, $2 \text{ km} \lesssim z \lesssim 3 \text{ km}$, the beam disintegrates into speckles with the most intense speckle forming OB. At larger distances, $z \gtrsim 3 \text{ km}$, OB amplitude fluctuates about approximately z -independent value $\langle I_{max}(z) \rangle$ as seen in Fig. 3b. According to Fig. 2, OB waist fluctuates about w_0 , so the optical power in OB is also approx-

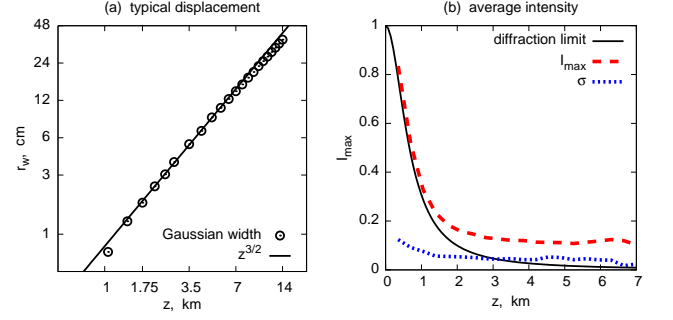


Fig. 3. (Color online) (a) Mean square displacement r_w from simulations (circles) vs. the accelerated random walk law $z^{3/2}$ (solid line). (b) Dashed line shows $\langle I_{max}(z) \rangle$ for OB averaged over 50 realizations with $I_{max}(z = 7\text{km}) \simeq 0.13$. Dotted line represents the standard deviation from $\langle I_{max}(z) \rangle$. Solid line shows $I_{max}(z)$ for diffraction-limited beam.

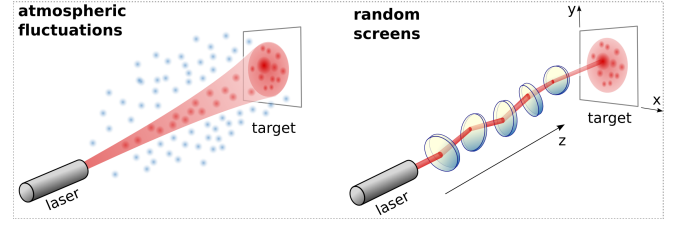


Fig. 4. (Color online) A sketch of laser beam propagation through random fluctuations of refraction index in turbulent atmosphere in strong irradiance fluctuation regime. Left panel: entire spread of beam is shown. Right panel: OB propagation is shown with scattering on random fluctuations at random screens interpreted as small lenses with random displacement, tilt and focal lengths.

imately constant at $z \gtrsim 3 \text{ km}$. Qualitatively we interpret this behavior as random multiple focusing-defocusing events of OB at random screens which compensate the diffraction in average.

To explain why the intensity profile of OB is close to Gaussian we recall that each random phase screen modifies ψ into $\psi e^{iS(\mathbf{r})}$. Neglecting the effect of small scale fluctuations of $S(\mathbf{r})$ on OB dynamics, we expand $S(\mathbf{r})$ near the center of OB into Taylor series as $S(\mathbf{r}) = S(\mathbf{r}_0) + (\mathbf{r} - \mathbf{r}_0) \cdot \nabla S(\mathbf{r}_0) + \sum_{l,m=1}^2 (1/2)(x_l - x_{l,0})(x_m - x_{m,0}) \nabla_l \nabla_m S(\mathbf{r}_0) + O(|\mathbf{r} - \mathbf{r}_0|^3)$, where $(x_1, x_2) \equiv (x, y)$ and $\nabla_l \equiv \partial/\partial x_l$. Each derivative of S is the Gaussian random variable. Then the linear term $(\mathbf{r} - \mathbf{r}_0) \cdot \nabla S(\mathbf{r}_0)$ ensures a small random reorientation of OB about z direction at each phase screen. The quadratic form $\sum_{l,m=1}^2 (1/2)(x_l - x_{l,0})(x_m - x_{m,0}) \nabla_l \nabla_m S(\mathbf{r}_0)$ can be diagonalized by the linear transform of $\mathbf{r} - \mathbf{r}_0$ and is responsible for the change of curvature of OB front. Both linear and quadratic terms can be qualitatively interpreted as multiple thin lenses located in the plane of each phase screen as schematically shown in Fig. 4. Linear terms are responsible for the random shift of the center of lenses in transverse plane or small tilt with respect

to the transverse plane. Either mechanism results in the random change of slopes and wander of OB in transverse direction as shown in Fig. 3a and Fig. 4. The quadratic terms can be interpreted as the action of multiple small focusings/defocusing lenses on the curvature of the OB front during propagation.

A general (non-Gaussian solution) of Eq. (1) for propagation between screens can be represented through the expansion in Hermite-Gaussian modes with the Gaussian beam being the zeroth mode of that expansion [24]. $O(|\mathbf{r} - \mathbf{r}_0|^3)$ term in $S(\mathbf{r})$ distorts the initial Gaussian beam by producing nonzero Hermite-Gaussian modes at each phase screen. These modes form ripples in $I(\mathbf{r})$ around the main beam so that the total optical power is conserved. During the initial propagation, $z \lesssim 3$ km, a fraction of optical power of these ripples that is returned to the main beam at each subsequent phase screen is small. This process continues until OB is formed which corresponds to the approximate statistical steady state for $z \gtrsim 3$ km. On these propagation distances, the small fraction of power lost from OB to higher Hermite-Gaussian modes at each random screen is approximately compensated by the power returned to OB from surrounding non-small ripples. This effect is however small between neighboring screens, which explains why OB needs to be close to Gaussian form with $w \simeq w_0$.

In conclusion, we found that OB carry $\gtrsim 21\%$ of initial power in 1 per 1000 realizations. One can identify optimal atmospheric realizations by a lower power laser beam which continuously illuminates target plane. When target camera/telescope detects an optimal realization on the target, it triggers the pulse operation of the high-power laser. The typical transverse displacement of OB is ~ 10 cm as seen in Fig. 3a. If higher precision of OB location is required, for instance for space-debris cleaning [10], then one, in addition, can continuously scan a lower power laser beam over angles to find optimal realization for transverse OB location.

Acknowledgments. The authors thank I.V. Kolokolov and V.V. Lebedev for helpful discussions. This work was supported by the National Science Foundation(NSF) grant DMS-1412140. Simulations were performed at the Texas Advanced Computing Center using the Extreme Science and Engineering Discovery Environment (XSEDE), supported by NSF Grant ACI-1053575.

References

- [1] J. W. Strohbehn, ed., *Laser Beam Propagation in the Atmosphere* (Springer, New York, 1978).
- [2] V. I. Tatarskii, *Wave Propagation in a Turbulent Medium* (McGraw-Hill Series in Electrical Engineering, New York, 1961).
- [3] V. I. Tatarskii, *The Effects of the Turbulence Atmosphere on Wave Propagation* (Jerusalem: Israel Program for Scientific Translations, Jerusalem, 1971).
- [4] L. C. Andrews and R. L. Phillips, *Laser Beam Propagation Through Random Media. Press Monograph Series vol PM53* (1998).
- [5] S. L. Lachinova and M. A. Vorontsov, “Giant irradiance spikes in laser beam propagation in volume turbulence: analysis and impact,” *J. Opt.* **18**, 025608 (2016).
- [6] S. N. Vlasov, V. A. Petrishchev, and V. I. Talanov, “Averaged description of wave beams in linear and nonlinear media,” *Izv. Vys. Uchebn. Zaved. Radiofizika* **14**, 1353 (1971).
- [7] V. E. Zakharov, “Collapse of langmuir waves,” *Sov. Phys. JETP* **35**, 908 (1972).
- [8] P. M. Lushnikov, S. A. Dyachenko, and N. Vladimirova, “Beyond leading-order logarithmic scaling in the catastrophic self-focusing of a laser beam in Kerr media,” *Phys. Rev. A* **88**, 013845 (2013).
- [9] P. M. Lushnikov and N. Vladimirova, “Non-gaussian statistics of multiple filamentation,” *Opt. Lett.* **35**, 1965–1967 (2010).
- [10] I. A. Vaseva, M. P. Fedoruk, A. M. Rubenchik, and S. K. Turitsyn, “Light self-focusing in the atmosphere: thin window model,” *Scientific Reports* **6**, 30697 (2016).
- [11] P. M. Lushnikov and N. Vladimirova, “Nonlinear combining of laser beams,” *Optics Letters* **39**, 3429–3432 (2014).
- [12] P. M. Lushnikov and N. Vladimirova, “Modeling of nonlinear combining of multiple laser beams in Kerr medium,” *Optics Express* **23**, 31120–31125 (2015).
- [13] A. Hasegawa and F. Tappert, “Transmission of stationary nonlinear optical pulses in dispersive dielectric fibers. I. Anomalous dispersion,” *Appl. Phys. Lett.* **23**, 142–144 (1973).
- [14] J. A. Fleck, J. R. Morris, and M. D. Feit, “Propagation of high-energy laser beams in the atmosphere,” *Appl. Phys.* **10**, 129–160 (1976).
- [15] M. S. Rytov, Y. A. Kravtsov, and V. I. Tatarskii, *Principles of Statistical Radiophysics 4: Wave Propagation through Random Media* (Springer-Verlag, Berlin, 1989).
- [16] W. Feller, *An Introduction to Probability Theory and Its Applications* (Wiley, New York, 1957).
- [17] I. M. Lifshitz, “The energy spectrum and the quantum states of disordered condensed systems,” *Usp. Fiz. Nauk* **83**, 617–663 (1964). [*Sov. Phys. Uspehi* 7 (4) 549-573 (1965)].
- [18] L. N. Lipatov, “Divergence of the perturbation-theory series and the quasiclassical theory,” *Zh. Eksp. Teor. Fiz.* **72**, 411–427 (1977). [*Sov. Phys. JETP* 45, 216–223 (1977)].
- [19] G. Falkovich, I. Kolokolov, V. Lebedev, and A. Migdal, “Instantons and intermittency,” *Phys. Rev. E* **54**, 4896 (1996).
- [20] M. Chertkov, “Instanton for randomvection,” *Phys. Rev. E* **55**, 2722 (1997).
- [21] T. Grafke, R. Grauer, , and T. Schafer, “The instanton method and its numerical implementation in fluid mechanics,” *J. Phys. A: Math. Theor.* **48**, 333001 (2015).
- [22] G. E. Falkovich, I. Kolokolov, V. Lebedev, and S. K. Turitsyn, “Statistics of soliton-bearing systems with additive noise,” *Phys. Rev. E* **63**, 025601(R) (2001).
- [23] Y. Chung and P. M. Lushnikov, “Strong collapse turbulence in quintic nonlinear schrödinger equation.” *Physical Review E* **84**, 036602 (2011).
- [24] A. E. Siegman, *Lasers* (University Science Books, Mill Valley, California, 1986).